



Cite this: *RSC Adv.*, 2018, 8, 7179

Efficient and reusable SBA-15-immobilized Brønsted acidic ionic liquid for the ketalization of cyclohexanone with glycol

Ruiyun Li,^{ab} Heyuan Song,^{ab} Guoqin Wang^{ab} and Jing Chen^{*a}

Ketalization of cyclohexanone with glycol has been carried out using molecular sieve SBA-15 immobilized Brønsted acidic ionic liquid catalyst. The properties of the heterogeneous catalysts were characterized by elemental analysis, Fourier transform infrared (FT-IR) spectra, scanning electron microscopy (SEM), thermogravimetry/differential scanning calorimetry (TG/DSC), and N₂ adsorption–desorption (BET). The results suggested that Brønsted acidic ionic liquid [BSmim][HSO₄] had been successfully immobilized on the surface of SBA-15 and the catalytic performance evaluation demonstrated that the catalyst BAIL@SBA-15 exhibited excellent catalytic activities in the ketalization of cyclohexanone with glycol. In addition, the effects of reaction temperature, catalyst loading, reaction time, and reactant molar ratio have also been investigated in detail, and a general reaction mechanism for the ketalization of cyclohexanone with glycol was given. The SBA-15 immobilized ionic liquid can be recovered easily and after reusing for 5 times in the ketalization reaction, the catalyst could still give satisfactory catalytic activity.

Received 16th December 2017

Accepted 26th January 2018

DOI: 10.1039/c7ra13385e

rsc.li/rsc-advances

1. Introduction

Currently, ionic liquids (ILs) are receiving widespread attention as media for a variety of reactions because of their unique properties such as low vapor pressure, high chemical and thermal stability, and adjustable structure.^{1–4} Compared to conventional acid catalysts, acidic ionic liquids possess several advantages, such as, reactions can be carried out under solvent-free conditions, and the physical and chemical properties of ionic liquids can be tailored by varying cations and anions.^{5,6} Since 2002 when Cole *et al.*⁷ first reported SO₃H-functionalized ionic liquids with strong Brønsted acidity, the applications of the Brønsted acidic ionic liquids (BAILs) with alkyl sulfonic acid groups in cations as a replacement for conventional homogeneous and heterogeneous acids have received great attention.^{7–10} And BAILs have been used as acid catalysts for esterification, alkylation, Pechmann reactions, acetalization and oligomerization.^{11–13}

Although ionic liquids have become commercially available, several drawbacks, such as unendurable viscosity, high cost and tedious purification procedure of the product, restricted their widespread applications.¹⁴ In order to solve problems mentioned above, immobilized ionic liquids catalysts combining the characteristics of ionic liquids, inorganic acids and solid acids had been proposed.^{15,16}

Compared to other well-known acid catalysts, immobilized ILs have several advantages. The most important may be the easily adjustable acidity, and the possibilities given by the selection of support materials.^{17,18} Recently, rapidly increasing reports have become available describing the application of task specific ionic liquids (TSILs) immobilized on various supports. The immobilized TSILs show additional advantages, such as decreasing consumption of ionic liquids, the facilitation of catalyst separation and recycling from reaction system, lower contamination of product, and the ability of using in gas phase reactions.¹⁹ In 2007, Sugimura *et al.*⁸ investigated the copolymerization of 1-vinylimidazolium based acidic ionic liquid with styrene and its use as effective and reusable catalyst for acetal formation under mild reaction condition. In 2011, Miao *et al.*¹⁷ reported acetalization of different aldehydes with alcohols catalyzed by SG-[(CH₂)₃SO₃H-HIM]HSO₄. The yields range from 85% to 98.5% under condition of 4 wt% catalyst amount, 110 °C. In 2004, a novel micropore zeolite MOR supported acidic ionic liquids was prepared.²⁰ It possesses an excellent performance for ketalization of cyclohexanone with glycol. The conversion of cyclohexanone can reach 69.5%.

More recently, it has reported on the preparations of a series of organic–inorganic hybrid mesoporous materials incorporated with ionic liquids.²¹ The commonly used solid supports may be subdivided into resins, nanotubes, fibers, zeolites and mesoporous silicas (MSs).²² Mesoporous materials possess the excellent characteristics of stable mesoporous structure, high surface area, controllable pore size, and thermal stability, which make them attractive supports for the preparation of immobilized ionic liquid catalyst.²³ Mesoporous materials, mostly

^aState Key Laboratory for Oxo Synthesis and Selective Oxidation, Lanzhou Institute of Chemical Physics (LICP), Chinese Academy of Sciences, Lanzhou, 730000, P. R. China. E-mail: chenj@licp.cas.cn; Fax: +86-931-496-8129; Tel: +86-931-496-8068

^bUniversity of Chinese Academy of Sciences, Beijing, 100049, P. R. China



ordered mesoporous molecular sieves (MCM-41, SBA-15), have been used as efficient catalysts and supports for many catalytic reactions.^{24–29} As an appealing type of mesoporous material, SBA-15 has relatively large specific surface area, controlled pore size and pore volumes. Besides, the abundant hydroxyl group on surface of SBA-15 could render it convenient for chemical modification and suitable for specific catalytic applications. Furthermore, the surface of the molecular sieves are sensitive to hydrothermal treatment, and the hydrothermal treatment could be used to activate the surface of SBA-15 and increase its capacity for grafting. Additives NaCl, KCl and NaF *etc.* are usually used to moderate the wall thickness and the degree of polymerization during post-synthesis hydrothermal treatments of SBA-15.^{30,31} All these make SBA-15 a potential candidate to act as suitable supports.^{32–35}

In these papers, a series of heterogeneous catalysts, mesoporous materials SBA-15 and amorphous SiO₂ immobilized SO₃H-functionalized ionic liquid was synthesized. And the surface properties of the obtained catalysts were characterized by elemental analysis, Fourier transform infrared (FT-IR) spectra, scanning electron microscopy (SEM), thermogravimetry/differential scanning calorimetry (TG/DSC) and N₂ adsorption-desorption isotherms (BET). Moreover, the effects of reaction parameters such as reaction time, reaction temperature and catalyst loading were studied and the recyclability of the catalyst was also examined. A general reaction mechanism for ketalization of cyclohexanone with glycol was given.

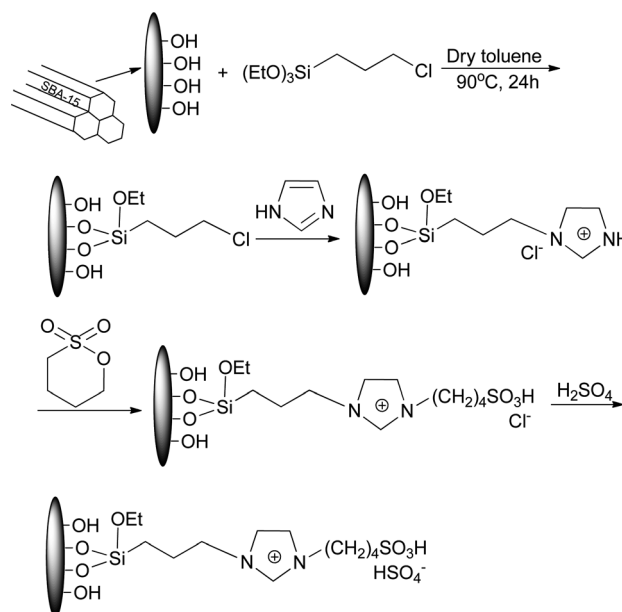
2. Experimental

2.1. Material

Silica gel (35–60 mesh) was purchased from Sigma-Aldrich. SBA-15 was purchased from Nanjing XFNANO Materials Tech Co., Ltd. 3-Chloropropyltriethoxysilane (CPES, purity ≥ 98%), 1,4-butane sultone (purity ≥ 99%) and 1-methylimidazole (purity ≥ 99%) was purchased from Aladdin Reagent Co, Ltd (Shanghai, China). Toluene, anhydrous ethanol, ethyl ether, anhydrous methanol, acetone, sulfuric acid were purchased from Rianlon Chemical Co., Ltd. Cyclohexanone and toluene were dried according to standard operations and stored over 4 Å molecular sieves. Other reagents were of analytical grade and used without any further purification.

2.2. Synthesis of [BSmim][HSO₄]

[BSmim][HSO₄] was synthesized and purified according to the literature.^{36,37} 1,4-Butane sultone (27.23 g, 0.2 mol) was dissolved in toluene, and 1-methylimidazole (16.42 g, 0.2 mol) was added dropwisely. The mixture was stirred at 60 °C for 8 h under vigorous stirring to obtain the white precipitate. The generated white solid zwitterion was filtrated and washed with toluene for three times. After dried in vacuum to remove unreacted materials, the zwitterion was mixed with H₂SO₄ in a molar ratio of 1 : 1 in anhydrous toluene, and stirred magnetically at 60 °C for 8 h. Finally, the mixture was dried in vacuum to form corresponding BAILS.



Scheme 1 Synthesis of [BSmim][HSO₄]@SBA-15.

2.3. Synthesis of SBA-15 immobilized ionic liquid

SBA-15 supported acidic ionic liquid was synthesized according to the literature.³⁸ Activated SBA-15 (5 g) was suspended in 50 ml dry toluene and an excess of 3-chloropropyltriethoxysilane (6 g) was added. The mixture was reacted under stirring for 24 h at 90 °C. Upon the reaction was completed, the products was collected by filtration and washed with toluene and ethyl ether in turn for three times. After dried under vacuum at 70 °C for 8 h, SBA-15-Cl was obtained as a white powder.

Subsequently, SBA-15-Cl (all product obtained from the last step) was placed in a reaction flask containing 50 ml toluene and an excess of imidazole (3 g) was added. The mixture was refluxed with stirring for 24 h at 90 °C. Then the products was disposed in the same way as the last step to acquire intermediate [SBA-15-im]Cl. The obtained [SBA-15-im]Cl and 1,4-butane sultone (4.0 g) were added in a 200 ml flask containing 50 ml toluene. The mixture was reacted with magnetic stirring for another 24 h at 100 °C, to undergo a condensation reaction to form the silica chemically bonded sultone. After the same treatment, [SBA-15-Bs-im]Cl was dried under vacuum at 60 °C for 8 h.

Finally, [SBA-15-Bs-im]Cl was added in a round-bottom flask containing 100 ml 1,2-dichloromethane. 1,2-Dichloromethane diluted 2.5 g of sulphuric acid was slowly added into the flask at 0 °C with stirring. The mixture was gradually heated to room temperature and reacted for 48 h. Then, the mixture was washed and filtered with 1,2-dichloromethane and ethyl ether until the pH of the filtrate reached 7.0. The prepared SBA-15 immobilized ionic liquid BAIL@SBA-15 was dried under vacuum at 60 °C for 12 h to remove the residual volatiles and moisture before use (Scheme 1).



2.4. Catalyst characterization

Elemental analysis was performed on an Elementar Vario EL cube analyzer (Elementar Analysensysteme GmbH, Germany) and the grafting amount of ILs on supports was determined by the contents of the N element. Fourier transform infrared (FT-IR) spectra in the frequency range of 4000–400 cm^{-1} were measured at room temperature on a Nexus 870 spectrometer (Nicolet Instruments Co., USA). Thermogravimetry/differential scanning calorimetry (TG/DSC) was performed on a Netzsch Model STA 449 F3 simultaneous thermal analyzer (Netzsch, Germany) in an air atmosphere. The shape and surface morphology of the catalysts were examined *via* scanning electron microscopy (SEM) (Model SU8020, Hitachi, Japan). N_2 adsorption–desorption isotherms were recorded using a TristarII 3020 instrument (Micromeritics, USA) and pore size distribution curves were calculated from the analysis of desorption branch of the isotherm by the BJH (Barrett–Joyner–Halenda). Before adsorption, samples were degassed at 473 K for 4 h.

2.5. Catalytic activity evaluation

Catalytic activity experiments were conducted in a 25 ml round-bottom flask. Immobilized ILs, cyclohexanone and glycol were added quantitatively into the reactor successively. The mixture was heated to a desired temperature and stirred at a speed of 600 rad min^{-1} . Upon reaction completion, the qualitative analysis of products was performed by Agilent 7980A/5975C GC-MS. The products were quantified by GC Smart equipped with a hydrogen flame ionization detector (FID). A capillary column ZB-WAX (30 m \times 0.25 mm \times 0.25 μm) was used to determine the composition of the samples with nitrogen as the carrier gas at a flow rate of about 3 ml min^{-1} . 1,2-Dichloroethane was used as the internal standard for the quantitative analysis of the products.

3. Results and discussion

3.1. FT-IR

To confirm the immobilization of active component on the mesoporous structure, FT-IR spectroscopic studies were carried out in the frequency range of 4000–400 cm^{-1} . The FT-IR spectra of molecular sieve SBA-15, amorphous SiO_2 and immobilized ionic liquids catalysts were shown in Fig. 1(a), respectively. As can be seen from the spectra of BAIL@SBA-15, the characteristic peaks of [Bsmim][HSO_4] around 3150 cm^{-1} , 2970 cm^{-1} , 1571 cm^{-1} , and 1176 cm^{-1} , 1058 cm^{-1} , 626 cm^{-1} , 525 cm^{-1} could be clearly observed. They were ascribed to N–H, C–H, C=C and C=N stretching vibrations of the imidazole ring, and S=O symmetric stretching vibrations of the SO_3H group and hydrogen sulfate, respectively.^{39,40} The typical peaks of Si–O–Si on SBA-15 supported ionic liquids could be observed around 460 cm^{-1} , 769 cm^{-1} and 954 cm^{-1} and the strong absorbance at 3440 cm^{-1} and 1630 cm^{-1} corresponds to the stretching frequency of physical adsorbed water. Hence, the above results confirm that the ILs were successfully immobilized onto the supports by covalent bonds.

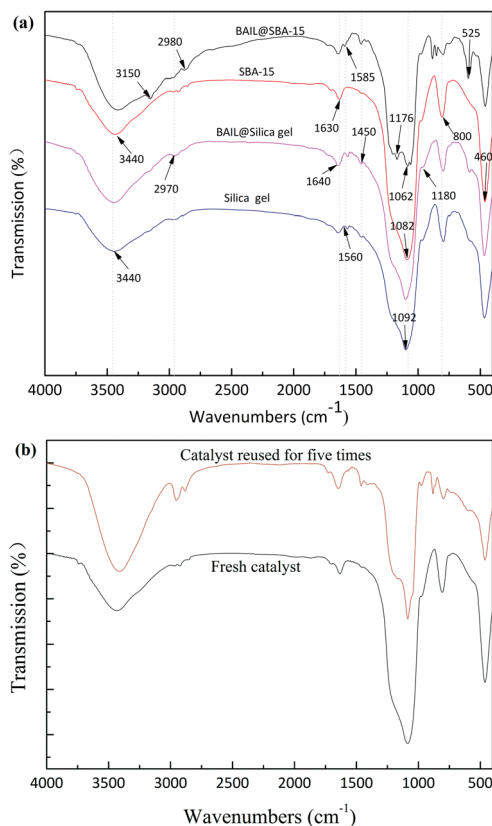


Fig. 1 Fourier transform infrared spectra of (a) molecular sieve and supported catalysts; and (b) the fresh and five times reused catalysts.

3.2. SEM

Fig. 2 shows the scanning electron microscopy (SEM) images of the samples. It can be seen from the pictures that samples are amorphous and accumulations of small particles. Compared with the catalyst in Fig. 2(b), the patent material in Fig. 2(a) is smoother than the former because of immobilization of the IL.

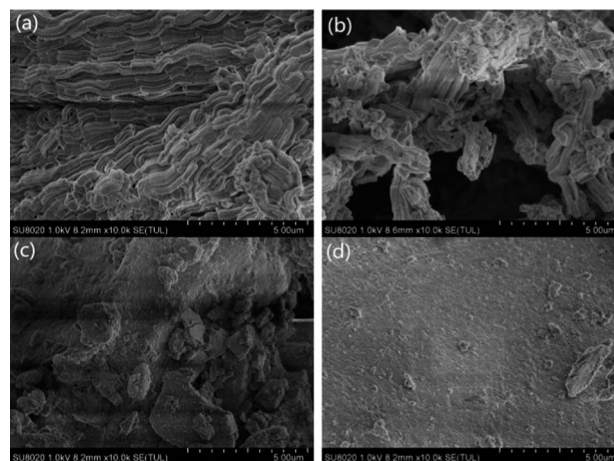


Fig. 2 SEM images of (a) BAIL@SBA-15; (b) SBA-15; (c) BAIL@Silica gel; (d) silica gel.



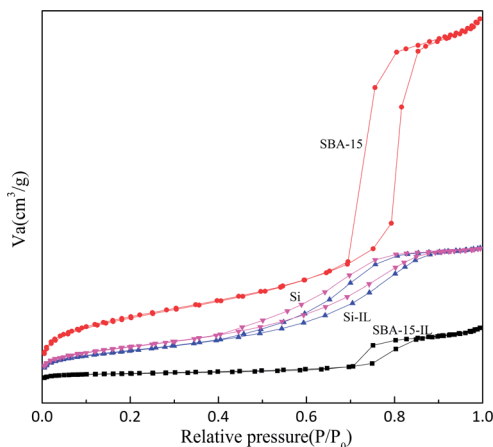


Fig. 3 N_2 adsorption–desorption isotherms of the catalysts.

Table 1 Physical properties of the supported ionic liquid

Samples	BET surface area, S_{BET} ($\text{m}^2 \text{g}^{-1}$)	Pore volume, V_p ($\text{cm}^3 \text{g}^{-1}$)	D_p (\AA)	Bonding amount (mmol g^{-1})
SBA-15	541.8	1.3	97.2	0
BAIL@SBA-15	42.9	0.2	125.2	1.5342
Silica gel	297.1	0.5	65.0	0
BAIL@Silica gel	262.9	0.4	73.8	0.4418

And the ionic liquid [Bsmim][HSO_4] had been immobilized on the surface of SBA-15.

3.3. N_2 adsorption–desorption

The N_2 adsorption–desorption isotherms and pore size distribution of the mesoporous materials and catalysts are depicted in Fig. 3. The textural properties such as the BET surface areas, pore diameter and pore volume derived from the N_2 adsorption–desorption measurements are included in Table 1. It is clear that the obtained isotherms are similar to type IV isotherm curve with H1-type hysteresis loop, characteristic of highly ordered mesoporous materials according to the IUPAC classification. Adsorption data were obtained over a relative pressure ranging from 0.01 Pa to 0.99 Pa. The BAIL@SBA-15 exhibits a hysteresis loop and a sharp increase in pore volume adsorbed above a relative pressure (P/P_0) at 0.7 Pa.

The physical properties of molecular sieve, silica gel and immobilized catalysts are shown in Table 1. Compared to parent mesoporous materials, the surface area of SBA-15 decreased from $541.8 \text{ m}^2 \text{g}^{-1}$ to $42.9 \text{ m}^2 \text{g}^{-1}$ with the increasing of pore size from 9.7 nm to 12.5 nm. This is attributed to the immobilization of BAIL onto the framework of molecular sieve. The immobilization of ionic liquids blocked a small fraction of the pores, which leads to the increasing of the average pore size and the aggregation of adjacent plate-like particles. The surface modification is probably a multi-layered process, in which additional ILs molecules interact with those covalent attached to the supports surface.

From all the above surface analysis data, it is confirmed that the 3-chloropropyl-triethoxysilane and ionic liquid is modified into the framework of the molecular sieve and amorphous silica.

3.4. TG-DSC

The TG-DSC analysis was employed to investigate the thermal stability of the catalysts. The thermograms of the samples are presented in Fig. 4. The thermogravimetric (TG) curve of BAIL@SBA-15 showed an initial weight loss of $\sim 10\%$ up to 100°C , which is attributed to the release of physisorbed water and residual solvent in supported catalysts. A significant weight loss of $\sim 30\%$ was found in the temperature range of $200\text{--}400^\circ\text{C}$ because of the organic components of ionic liquid and the propyl of 3-chloropropyltriethoxysilane separated from the surface of support. The peaks in the DSC curve also prove this process. Therefore, the catalysts can be operated stably under 100°C (Table 1).

3.5. Ketalization of cyclohexanone with glycol

The catalytic activity of several supported ILs were evaluated on the ketalization of cyclohexanone with glycol under the optimized reaction condition and the results were listed in Table 2. It can be observed that the molecular sieve SBA-15 as catalyst has 22.6% conversion of cyclohexanone (CYC), which demonstrates molecular sieve SBA-15 has relatively poor catalytic activity (Table 2, entry 4). With the successful immobilization of ionic liquid [Bsmim][HSO_4] on molecular sieve, the BAIL@SBA-15 gave a drastic increase in the catalytic activity and the conversion of cyclohexanone was 85.2% (Table 2, entry 1). However, there is little inferior to the corresponding homogeneous catalyst of [Bsmim][HSO_4] (Table 2, entry 3) under the same condition. The heterogeneous catalyst BAIL@SBA-15 can remain high catalytic performance, even though the catalyst loading content of Brønsted acidic ionic liquid was obviously less than the pure BAIL. Therefore, the molecular sieve SBA-15 plays a significant roles on the immobilized catalyst. The cooperative pathway of catalyst system enhances the conversion of cyclohexanone in the ketalization reaction. It could also be found that the SBA-15 supported acidic ionic liquid has much higher activity than the support materials of silica gel.

3.6. Influence of reaction parameters on the ketalization

SBA-15 supported acidic ionic liquid was selected as catalyst in the ketalization reaction to optimize the reaction condition since BAIL@SBA-15 showed excellent catalytic activity. The effect of reaction parameters such as reaction temperature, reaction time, catalyst loading, reactant molar ratio were investigated.

3.6.1. Effect of reaction temperature. The effect of reaction temperature was performed in the presence of BAIL@SBA-15 at 30°C , 40°C , 50°C , 60°C , 70°C . As shown in Fig. 5, the conversion of cyclohexanone increased from 73.9% to 85.2% when the reaction temperature increased from 30°C to 50°C . And the conversion of cyclohexanone increased rapidly when the temperature is lower than 50°C and slowly after 50°C . A reasonable explanation for this



observation may be that the ketalization reaction is an endothermic reaction and reached equilibrium at 50 °C. Therefore, 50 °C is the optimum reaction temperature.

3.6.2. Effect of catalyst loading. The conversion of cyclohexanone increased significantly when the catalyst loading is lower than 1.3% (Fig. 6), which means that increase of catalyst loading is conducive to the ketalization reaction. It can be seen that the conversion of cyclohexanone was enhanced with the increasing of the catalyst loading content from 0.33% to 1.3%. However, there is little change in the conversion of cyclohexanone when the amount of catalyst was increased from 1.3% to 3.9%. This implies that further increase in the amount of catalyst is not necessary for the conversion of cyclohexanone. Therefore, the preferable catalyst loading content of supported catalyst is 1.3%.

Table 2 Ketalization of cyclohexanone with glycol^a

Entry	Catalyst	Conversion of CYC/(%)	Selectivity/(%)
1	BAIL@SBA-15	85.2	100
2	BAIL@Silica gel	79.1	100
3	[BSmim][HSO ₄] ^b	88.7	100
4	SBA-15	22.6	100
5	Blank	0.5	100

^a Reaction conditions: cyclohexanone (30 mmol), glycol (60 mmol), catalyst (1.3%, based on the mole ratio of cyclohexanone), reaction temperature (50 °C), reaction time 3 h. ^b The molar ratio of [BSmim][HSO₄] is 10%.

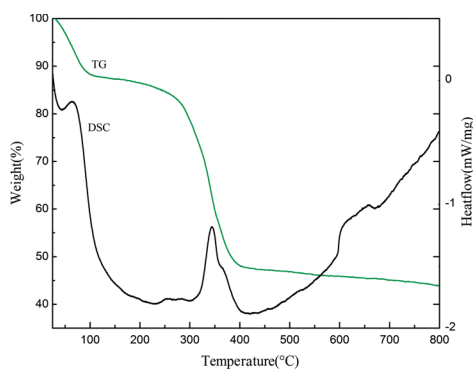


Fig. 4 TG-DSC curves of supported ILs (a) BAIL@SBA-15; (b) BAIL@Silica gel.

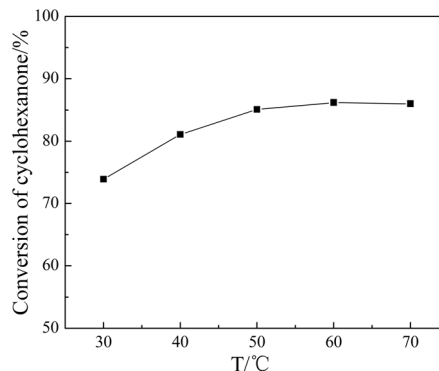


Fig. 5 Effect of reaction temperature on the conversion of cyclohexanone. Reaction conditions: $n(\text{EG}) : n(\text{CYC}) = 2$, $n(\text{IL}) : n(\text{CYC}) = 1.3\%$, 3 h.

3.6.3. Effect of reaction time. In order to study the reaction time on the ketalization reaction, the experiment was performed taking reaction time ranging from 0.5 h to 5 h. As can be seen from Fig. 7, the conversion of cyclohexanone increases from 40.9% to 85.1% by increasing the reaction time from 0.5 h to 3 h. Extending reaction time to 5 h, the conversion of cyclohexanone increased to 86.4%. Hence, it is not practical to promote the conversion of cyclohexanone by prolonging reaction time and the required time to reach the equilibrium is 3 h.

3.6.4. Effect of reactant molar ratio. The effect of the molar ratio of ethylene glycol (EG) to cyclohexanone (CYC) in the range of 1.0 to 2.5 on the conversion of cyclohexanone was shown in Fig. 8. It can be seen that the conversion of cyclohexanone is sensitive to the reactant molar ratio. With EG : CYC increased from 1 : 1 to 2 : 1, the conversion of cyclohexanone was enhanced from 58.1% to 85.1%. However, further increase of the molar ratio to 2.5 : 1 resulted in a decrease in conversion due to the reduction of catalyst concentration. Thus the most suitable molar ratio of EG : CYC was 2 : 1.

3.7. Mechanism

The possible mechanism for hydrogen bond between anion of ionic liquid and support was shown in Scheme 2. The supported

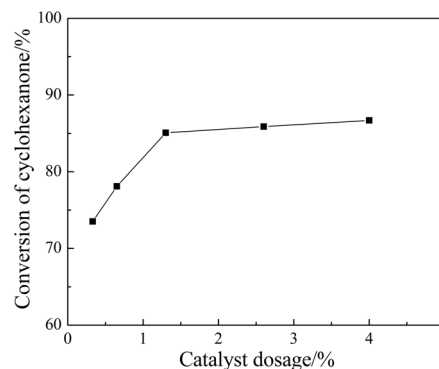


Fig. 6 Effect of catalyst dosage on the conversion of cyclohexanone. Reaction conditions: $n(\text{EG}) : n(\text{CYC}) = 2$, 3 h, 50 °C.



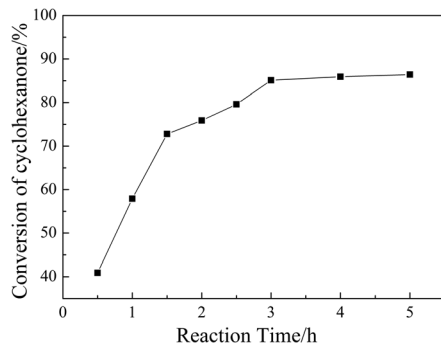


Fig. 7 Effect of reaction time on the conversion of cyclohexanone. Reaction conditions: $n(\text{EG}) : n(\text{CYC}) = 2$, $n(\text{IL}) : n(\text{CYC}) = 1.3\%$, $50\text{ }^\circ\text{C}$.

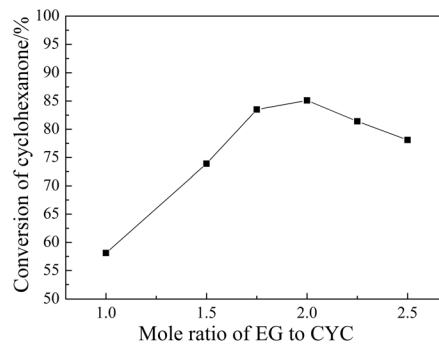
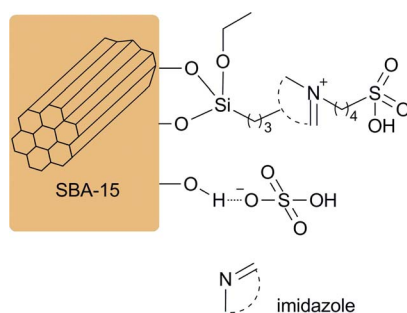


Fig. 8 Effect of catalyst dosage on the conversion of cyclohexanone. Reaction conditions: $n(\text{IL}) : n(\text{CYC}) = 1.3\%$, 3 h , $50\text{ }^\circ\text{C}$.



Scheme 2 The possible mechanism for hydrogen bond between anion of ionic liquid and support.

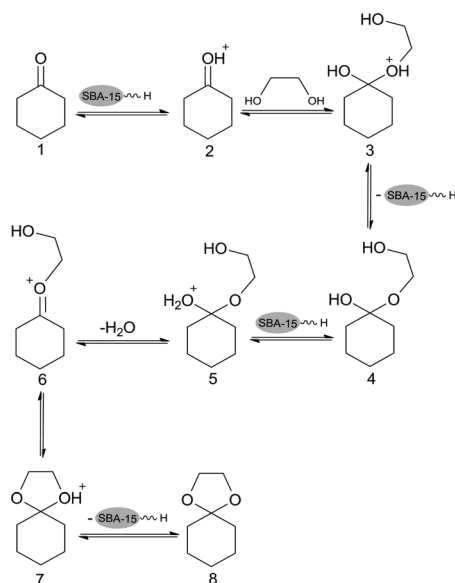
ionic liquids catalyst system is likely operated in a cooperative pathway. Cation of ionic liquid was firmly immobilized through the covalent bonds to the surface of the supports and the anion was also not easily lost because of ionic bonding with cation and

hydrogen bonding with supports. Therefore, the supported ionic liquid can be reused for several times with small loss in the selectivity and cyclohexanone conversion.

Ketalization is a reversible reaction and the possible two-step mechanism for ketalization of cyclohexanone with glycol over BAIL@SBA-15 was consistent with the reported ones.^{17,41} Scheme 3 envisages the mechanism of the ketalization of cyclohexanone with glycol using SBA-15 supported ionic liquid. In the first step, the cyclohexanone is protonated by the acid site of BAIL@SBA-15 (H^+ ions of the catalyst) to produce the intermediate 2 and then activated for nucleophilic addition of O atom of the alcohol to form the hemiacetal 4. Protonation of 4 leads to intermediate 5 which undergoes subsequent dehydration to give 6. It accepted a second molecule of alcohol hydroxyl group to give intermediate 7. This step is also an exothermic reaction, and last, removal of a proton from 7 leads to the formation of the ketal 8.

3.8. Recycling of catalyst

The recovery of catalyst is highly preferable from both environmental and economic points of view. The reusability of the SBA-15 supported ionic liquid was investigated in the ketalization of cyclohexanone with glycol, and the result was shown in Fig. 9. In each cycle, the catalyst was easily recovered by centrifugation and washed with dichloromethane for three



Scheme 3 General reaction mechanism for the ketalization of cyclohexanone with glycol.

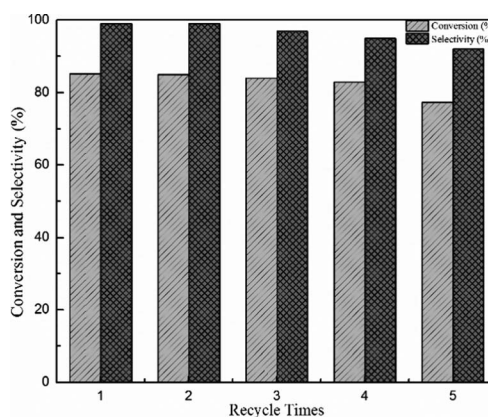


Fig. 9 The recycle test of BAIL@SBA-15 in the ketalization of cyclohexanone with glycol.



times, followed by drying under vacuum before the next run. As shown in Fig. 9, the catalyst BAIL@SBA-15 can be readily recovered and reused five times without significant loss of activity. And the conversion and selectivity were 77.4% and 92.0%, respectively.

The recovered catalyst that reused for five times has no obvious change in structure, referring to the FT-IR spectrum in comparison with fresh catalyst listed in Fig. 1(b). Measuring by elemental analysis, the grafting amount of ionic liquid on BAIL@SBA-15 decreased from 1.5342 mmol g⁻¹ to 0.4820 mmol g⁻¹ after being used for 5 times. It was found that the loss of anion HSO₄⁻ may be the main reason for the decrease in catalytic activity.

4. Conclusions

In summary, a series of mesoporous materials SBA-15 and amorphous SiO₂ supported acidic ionic liquids were synthesized by chemical covalent bond. On the basis of characterization results, the Brønsted acidic ionic liquid [Bsmim][HSO₄] was proved to be successfully immobilized onto mesoporous materials and the results show that BAIL@SBA-15 is more active in the ketalization reaction. The conversion of cyclohexanone can reach 85.2% and the amount of catalyst is reduced greatly compared with pure ionic liquids. The experiment demonstrated that the optimum reaction conditions for the ketalization of cyclohexanone with glycol is 1.3% of BAIL@SBA-15 as catalyst, initial molar ratio of EG : CYC was 2 and reaction temperature is 50 °C for 3 h. The possible mechanism for hydrogen bond between anion of ionic liquid and support and general reaction mechanism for ketalization reaction was given. Furthermore, the supported ionic liquids can be easily recovered for five times without a significant loss of catalytic activity.

Conflicts of interest

There are no conflicts to declare.

Acknowledgements

We gratefully acknowledge the National Natural Science Foundation of China (No. 21473225).

Notes and references

- 1 Y. Y. Jiang, G. N. Wang, Z. Zhou, Y. T. Wu, J. Geng and Z. B. Zhang, *Chem. Commun.*, 2008, 505–507.
- 2 D. Kuang, S. Uchida, R. Humphry-Baker, S. M. Zakeeruddin and M. Gratzel, *Angew. Chem.*, 2008, **47**, 1923–1927.
- 3 A. S. Amarasekara, *Chem. Rev.*, 2016, **116**, 6133–6183.
- 4 D. Fang, K. Gong, Q. Shi and Z. Liu, *Catal. Commun.*, 2007, **8**, 1463–1466.
- 5 H. Xing, T. Wang, Z. Zhou and Y. Dai, *J. Mol. Catal. A: Chem.*, 2007, **264**, 53–59.
- 6 T. Welton, *Coord. Chem. Rev.*, 2004, **248**, 2459–2477.
- 7 A. C. Cole and J. L. Jensen, *J. Am. Chem. Soc.*, 2002, **124**, 5962–5963.
- 8 R. Sugimura, K. Qiao, D. Tomida and C. Yokoyama, *Catal. Commun.*, 2007, **8**, 770–772.
- 9 H. H. Wu, F. Yang, P. Cui, J. Tang and M. Y. He, *Tetrahedron Lett.*, 2004, **45**, 4963–4965.
- 10 X. Liang and C. Qi, *Catal. Commun.*, 2011, **12**, 808–812.
- 11 J. P. Hallett and T. Welton, *Chem. Rev.*, 2011, **111**, 3508–3576.
- 12 P. Wasserscheid, M. Sessing and W. Korth, *Green Chem.*, 2002, **4**, 134–138.
- 13 J. P. B. Atef Arfan, *Org. Process Res. Dev.*, 2005, **9**, 743–748.
- 14 S. Sahoo, P. Kumar, F. Lefebvre and S. B. Halligudi, *Appl. Catal., A*, 2009, **354**, 17–25.
- 15 C. Feher, E. Krivan, J. Hancsok and R. Skoda-Foeldes, *Green Chem.*, 2012, **14**, 403–409.
- 16 W. Chen, Y. Zhang, L. Zhu, J. Lan, R. Xie and J. You, *J. Am. Chem. Soc.*, 2007, **129**, 13879–13886.
- 17 J. Miao, H. Wan, Y. Shao, G. Gua and B. Xu, *J. Mol. Catal. A: Chem.*, 2010, **348**, 77–82.
- 18 P. Sharma and M. Gupta, *Green Chem.*, 2015, **17**, 1100–1106.
- 19 Z. Wu, Z. Li, G. Wu, L. Wang, S. Lu, L. Wang, H. Wan and G. Guan, *Ind. Eng. Chem. Res.*, 2014, **53**, 3040–3046.
- 20 Z. M. Li, Y. Zhou, D. J. Tao, W. Huang, X. S. Chen and Z. Yang, *RSC Adv.*, 2014, **4**, 12160–12167.
- 21 H. Jin, M. B. Ansari and S. E. Park, *Catal. Today*, 2015, **245**, 116–121.
- 22 M. Wysocka-Zolopa, I. Zablocka, A. Basa and K. Winkler, *Chem. Heterocycl. Compd.*, 2017, **53**, 78–86.
- 23 Y. Wan and D. Zhao, *Chem. Rev.*, 2007, **107**, 2821–2860.
- 24 W. Xie and C. Zhang, *Food Chem.*, 2016, **211**, 74–82.
- 25 B. Lebeau, A. Galarneau and M. Linden, *Chem. Soc. Rev.*, 2013, **42**, 3661–3662.
- 26 K. A. Shah, J. K. Parikh and K. C. Maheria, *Catal. Today*, 2014, **237**, 29–37.
- 27 H. Zhao, N. Yu, Y. Ding, R. Tan, C. Liu, D. Yin, H. Qiu and D. Yin, *Microporous Mesoporous Mater.*, 2010, **136**, 10–17.
- 28 S. Udayakumar, S. W. Park, D. W. Park and B. S. Choi, *Catal. Commun.*, 2008, **9**, 1563–1570.
- 29 Z. Allothman, *Materials*, 2012, **5**, 2874–2902.
- 30 F. Zhang, Y. Yan, H. Yang, Y. Meng, C. Yu, B. Tu and D. Zhao, *J. Phys. Chem. B*, 2005, **109**, 8723–8732.
- 31 C. Pirez, A. F. Lee, J. C. Manayil, C. M. A. Parlett and K. Wilson, *Green Chem.*, 2014, **16**, 4506–4509.
- 32 J. N. Appaturi, M. R. Johan, R. J. Ramalingam and H. A. Al-Lohedan, *Microporous Mesoporous Mater.*, 2018, **256**, 67–74.
- 33 D. Zhao, J. Sun, Q. Li and G. D. Stucky, *Chem. Mater.*, 2000, **12**, 275–279.
- 34 J. Qin, B. Li and D. Yan, *Crystals*, 2017, **7**, 89–100.
- 35 K. Arya, D. S. Rawat and H. Sasai, *Green Chem.*, 2012, **14**, 1956–1963.
- 36 W. Wang, L. Shao, W. Cheng, J. Yang and M. He, *Catal. Commun.*, 2008, **9**, 337–341.
- 37 Y. Gu, F. Shi and Y. Deng, *Catal. Commun.*, 2003, **4**, 597–601.
- 38 J. Yang, T. Zeng, D. Cai, L. Li, W. Tang, R. Hong and T. Qiu, *Asia-Pac. J. Chem. Eng.*, 2016, **11**, 901–909.
- 39 K. Qiao, H. Hagiwara and C. Yokoyama, *J. Mol. Catal. A: Chem.*, 2006, **246**, 65–69.
- 40 Z. Xu, H. Wan, J. Miao, M. Han, C. Yang and G. Guan, *J. Mol. Catal. A: Chem.*, 2010, **332**, 152–157.
- 41 B. Thomas, S. Prathapan and S. Sugunan, *Microporous Mesoporous Mater.*, 2005, **80**, 65–72.

